Verification of measures to mitigate lightning current flowing into metal sheaths of power cables

Kazuo Yamamoto, Yuya Toriyama and Javier Herrera-Murcia

***Abstract*-- The power interconnection cables are sometime damaged in a wind farm when lightning strikes a wind turbine. This paper presents the verification of measures to mitigate lightning current flowing into metal sheaths of power cables. First, the transient ground characteristics and the transient characteristics of lightning current distributions at the target wind turbines were obtained by impulse tests, and an analysis model was constructed using a transient analysis program (ATP). The model mainly consists of a grounding system represented as an equivalent network obtained from a vector fitting routine, and a cable model represented as a JMarti frequency-dependent line. The results show that the transient ground characteristics and the lightning current transient characteristics are well reproduced. In addition, the effect of the grounding wires to mitigate the lightning current flowing into the cable sheath when the two wind turbines are concatenated by power cable sheath is also discussed.**

***Keywords*: Wind Turbine, Lightning, Grounding, Power cable, ATP, Vector fitting.**

I. Introduction

In recent years, increasing carbon dioxide emissions have become a serious social issue as a cause of energy resource depletion and global warming. For this reason, the introduction of renewable energy that does not emit carbon dioxide during power generation is progressing. Wind power generation systems are rapidly becoming popular due to their high energy conversion efficiency and large economies of scale [1].

On the other hand, there have been more than a few reports of damage to wind power generation systems, such as breakdowns and shutdowns, caused by natural phenomena such as typhoons, earthquakes, and lightning strikes. When lightning strikes the receptor of a wind turbine blade, it propagates through the lead in conductors within the blade, the nacelle structure, the tower, and the foundation, and the lightning current is released to the ground through the wind turbine grounding system [2], [3]. When the lightning current is released, the ground potential of the wind turbine rises, and overvoltage is applied to the equipment inside and outside the wind turbine. Electrical and electronic equipment inside and outside the wind turbine may fail due to this overvoltage. In addition, the power cable sheaths connected to the wind turbine grounding systems are sometime damaged due to part of the lightning current flowing into the sheaths [4]. To study the magnitudes and effects of this current and to design possible countermeasures against such incidents, it is important to understand the characteristics of the wind turbine grounding system and the shunt current flowing into the shield layer of the power cable.

In this study, the transient grounding characteristics of wind turbines and the transient characteristics of lightning currents flowing into grounding wires using vinyl-insulated conductors were obtained through impulse tests. Incidentally, these tests were conducted with both ends of the power cable sheath not connected to the wind turbine grounding systems. After the tests, analytical models capable of reproducing these characteristics were constructed using ATP [5]. Each grounding system of wind turbines is incorporated into the overall circuit as an equivalent network obtained through the Vector Fitting method [6]. The cable model is based on manufacturer information and installation conditions using the JMarti frequency-dependent model.

II. Experiments Of Wind Turbine Grounding Systems

A. The ground resistivity

A method for measuring ground resistivity is the Wenner method. It is a method of understanding the electrical structure of the ground by passing a current through the ground and measuring the potential difference and analyzing the results. Measurements are made using the arrangement shown in Fig. 1. Each electrode is driven into the ground at intervals of a [m], and a power source is connected to electrodes C1 and C2, and a voltage is applied between the electrodes to measure the potential difference between electrodes P1 and P2. The ground resistivity is determined equation (1) from the measured resistance value R [Ω], which is determined from the injected current I [A] and the potential difference value V [V]:

$$\rho = 2\pi aR \tag{1}$$

From measurements at electrode spacing a in Fig. 1, the average ground resistivity ρ at a depth of approximately a can be estimated.

Fig. 2 shows the representative values of ground resistivity around wind turbines No. 1 and No. 2. The layer structure shown in Fig. 2 was approximated using the experimental results obtained using the Wenner method, with an RMS error of approximately 10 Ωm.

Kazuo Yamamoto and Yuya Toriyama are with the Department of Electrical Engineering, Chubu University, Aichi, Japan
(e-mail: kyamamoto@isc.chubu.ac.jp).

Javier Herrera-Murcia is with the Department of Electrical Engineering, Universidad Nacional de Colombia, Colombia
(e-mail: jherreram@unal.edu.co).

Paper submitted to the International Conference on Power Systems Transients (IPST2025) in Guadalajara, Mexico, June 8-12, 2025.

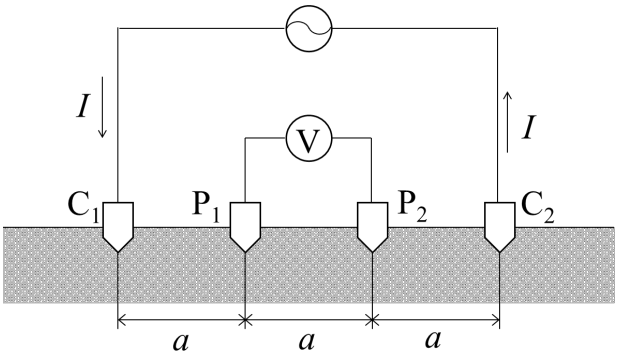

Fig. 1. Wenner method

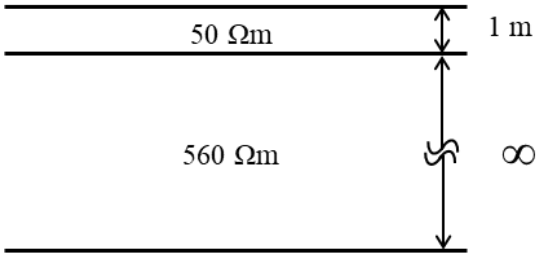

Fig. 2. Measured result of ground resistivity around the wind turbine

B. Transient grounding characteristics of single wind turbines No. 1 and No. 2

The capacitor (Rated voltage 2.5 kV, capacity 8 μF) was charged at 1 kV using the discharge function of the insulation resistance tester, and the measurement was performed using the IG (Impulse Generator, Fig. 3) including the charged capacitor, which discharges manually [7]. Fig. 4 shows a detailed diagram of the experimental circuit.

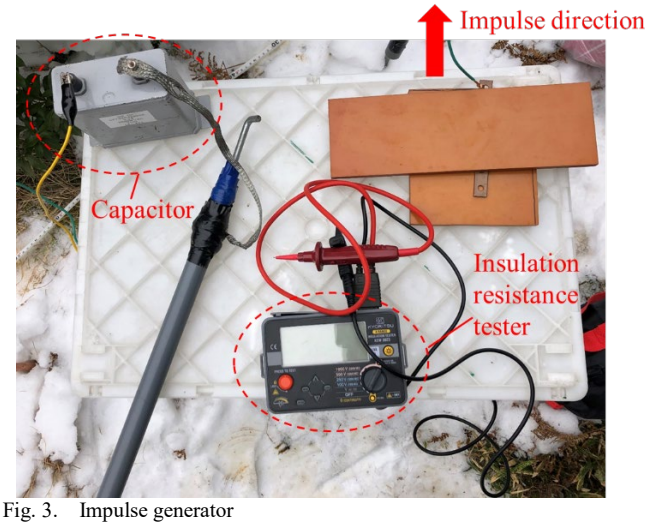

Fig. 3. Impulse generator

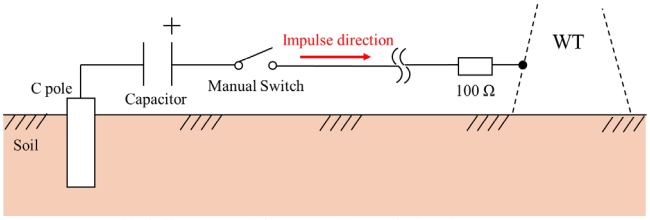

Fig. 4. Detailed diagram of the experimental circuit

In this experiment, current is injected into the wind turbine through a 100 Ω resistor connected between the current injection wire and the wind turbine. The voltage measuring electrode is installed 55 m away from the wind turbine, and the voltage measuring wire is extended to the wind turbine using IV wire. When current is injected into the wind turbine, the potential difference generated between the wind turbine and the voltage measuring wire is measured. Fig. 5 shows the experimental layout for a single wind turbine.

In this experiment, the grounding resistance of the IG is approximately 300 Ω to 400 Ω, which affects the maximum value of the injected current. However, the grounding resistance of the wind turbine is only a few ohms, and the current is injected through a 100 Ω resistor (which is significantly larger than the wind turbine grounding resistance), the IG can be considered equivalent to a current source. Therefore, if the grounding electrode of the IG is placed sufficiently far from the wind turbine foundation (typically more than 50 m), it will not affect the grounding characteristics of the wind turbine.

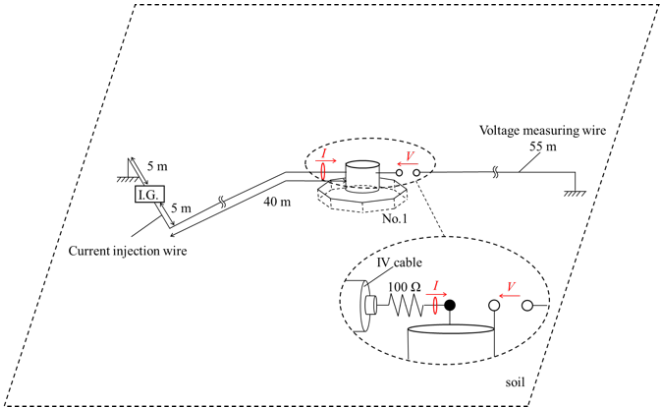

(a) Wind turbine No.1

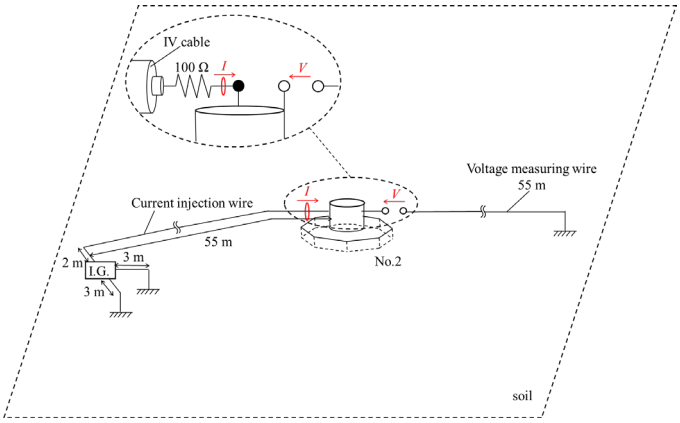

(b) Wind turbine No.2

Fig. 5. Experimental layout for a single wind turbine

C. Transient grounding characteristics of connected wind turbines No.1 and 2

The measurement conditions are shown in Fig. 6. The grounding systems of the wind turbine No.1 and No.2 are connected by the grounding wire (60 mm^2), then the current was injected into the foundation of No.1 using the IG. The grounding wire extends 290 m along the ground surface. At

that time, the potential rise waveform of wind turbine No. 1 and the shunt current waveform flowing into the ground wire connected to the wind turbine foundation were measured [7].

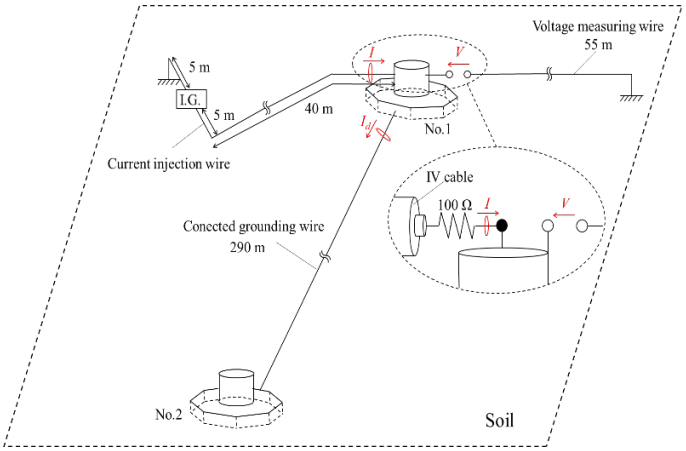

Fig. 6. Experimental layout for connected wind turbines

III. ATP Model Development

This section describes the development of the ATP model components. Based on the results obtained in Chapter II, the model reproduces the transient grounding characteristics of the wind turbine and the characteristics of the lightning current flowing in the grounding wire.

A. Grounding system models of each wind turbine

Models of the grounding systems of wind turbines No.1 and No.2 were synthesized into electrical networks from full-wave simulations based on experimental results and vector fitting routines. Using these methods, all the complex grounding systems can be converted into equivalent circuits that can be included in the ATP program.

As presented in [8] and [9] a grounding system exhibits a frequency response whose behavior depends on the surrounding ground parameters and its frequency dependence, the grounding system geometry and the materials involved in its construction. This frequency response can be evaluated theoretically or experimentally. Usually, the input impedance or admittance are obtained as seen from the connection point to the rest of the network and as a relation between the injected current and the measured voltage to a remote ground; in this work, the voltage and current waveforms obtained from the experimental results were transformed into the frequency domain and used to obtain the admittance function of the grounding system for a defined frequency band.

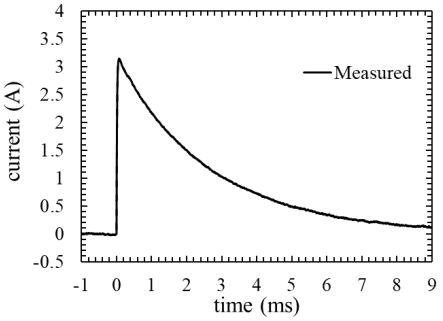

(a) Time response

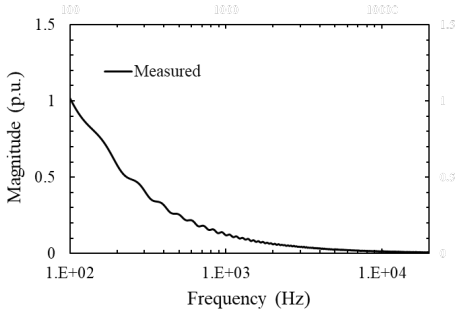

(b) Frequency – Magnitude Response

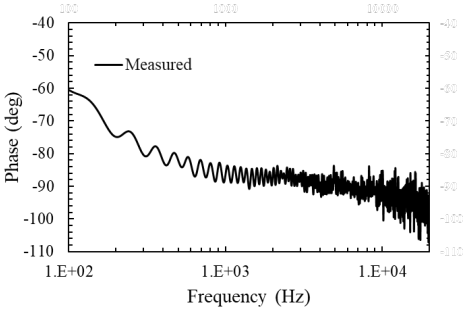

(c) Frequency – Phase Response

Fig. 7. Frequency characteristics of the current injected into No. 1.

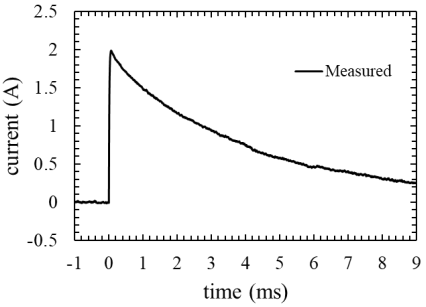

(a) Time response

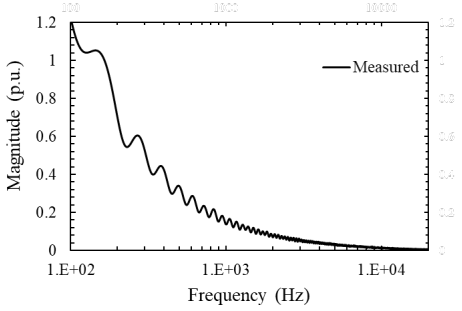

(b) Frequency – Magnitude Response

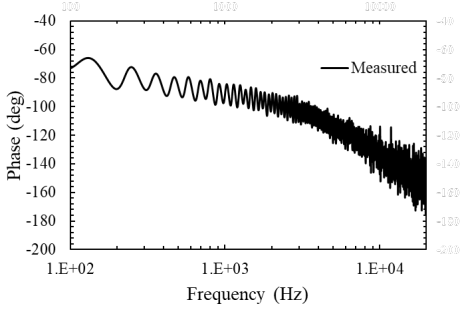

(c) Frequency – Phase Response

Fig. 8. Frequency characteristics of the current injected into No. 2.

To derive an equivalent network from the admittance and phase functions, a vector fitting routine was employed [6]. As stated in [10], truncation of the time-domain function and transformation to the frequency domain typically result in the need for many poles for function fitting. The time and frequency characteristics of the injected current for No. 1 and No. 2 are shown in Fig. 7 and Fig. 8. As is evident from these figures, the primary frequency components contained in the injected current are below 20 kHz. Therefore, the analysis model is designed to accommodate high-frequency characteristics up to 20 kHz, based on the characteristics of the injected current used in the experiment.

Some subsequent lightning strokes contain lightning currents with a wavefront of approximately 0.1 μs. To accurately analyze the characteristics of such currents when they flow into the grounding system, higher-frequency characteristics are required.

A total of 256 poles were required to fit the admittance response. It is important to note that the process of finding an adequate match between the vector fitting results and the measurements involves the variation of the initial and total number of the poles, the type of model (strictly proper, proper or improper) and the maximum frequency considered. Besides, even if a low error and stable fit is obtained, the model could violate some passivity constraints making the time-domain simulations unstable. Because of this, the model presented here was the best found among all the variations considered.

The results of the magnitude fitting process for the admittance and phase functions are shown in Fig. 9 and 10.

Based on this fitting procedure, a passivity forcing procedure [11] was applied to obtain an equivalent network from the fitted rational functions, which was then incorporated as an external library in the ATP program. The time-domain response of this equivalent network is compared with the experimental results in Fig.11 and Fig.12.

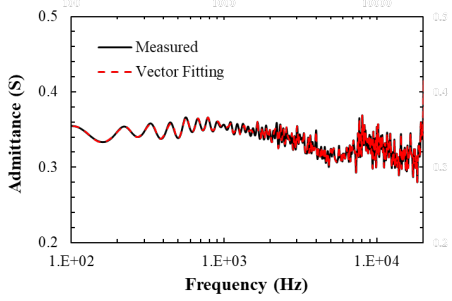

(a) Frequency – Magnitude Response

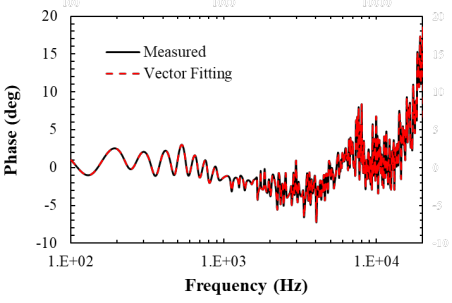

(b) Frequency – Phase Response

Fig. 9. Vector Fitting results of Wind turbine No.1

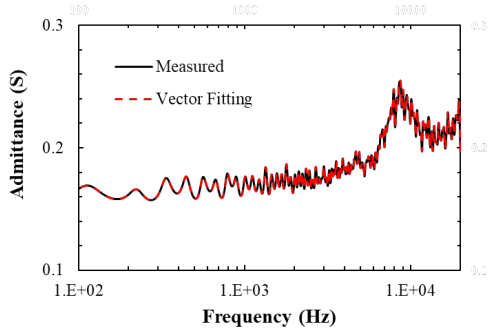

(a) Frequency – Magnitude Response

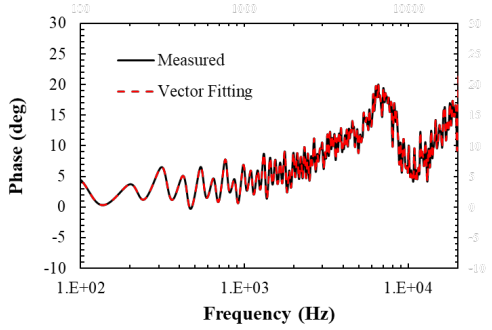

(b) Frequency – Phase Response

Fig. 10. Vector Fitting results of Wind turbine No.2

The comparison between Fig. 11 and Fig. 12 shows that the injected current waveforms and potential rise waveforms obtained from the analysis are in good agreement with the experimental results, confirming that the model was constructed appropriately. In addition, when the steady-state ground resistance values were calculated from the wave tail, it was confirmed that R_1 = 0.6 V / 0.1 A = 6.0 Ω for No. 1 and R_2 = 1.9 V / 0.25 A = 7.6 Ω for No. 2.

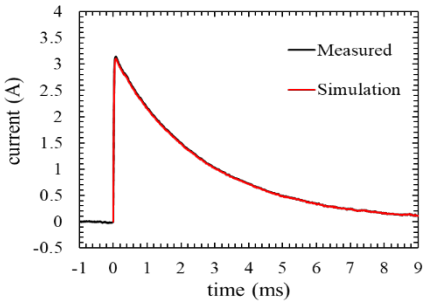

(a) Injection current waveform

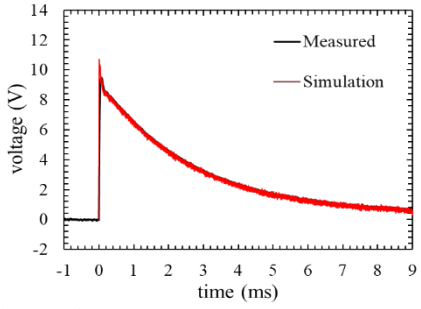

(b) Potential rise waveform

Fig. 11. Comparison of experimental results and analysis results when current is injected into the single model of the wind turbine No. 1.

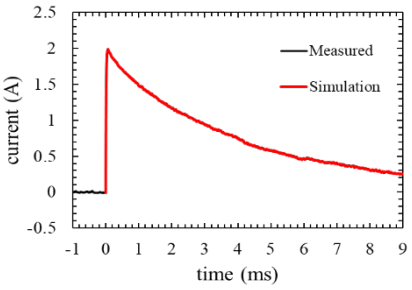

(a) Injection current waveform

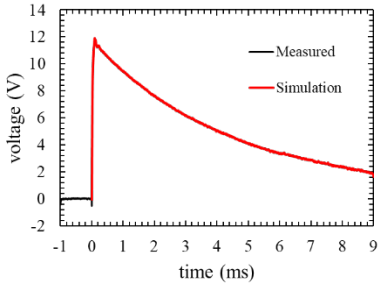

(b) Potential rise waveform

Fig. 12. Comparison of experimental results and analysis results when current is injected into the single model of the wind turbine No. 2.

Fig. 11 and 12, the potential rise characteristics were experimentally obtained when injecting a long-tail current, and these experimental results were used to construct individual analysis models for Wind Turbines No. 1 and No. 2. This approach enables the development of a highly accurate analysis model that includes low-frequency characteristics (steady-state characteristics) as well as the high-frequency characteristics.

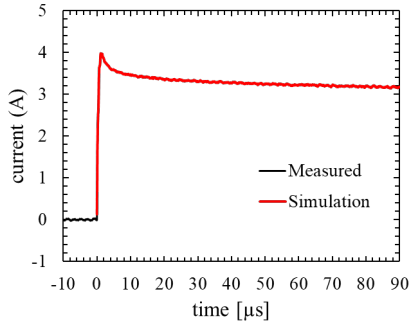

(a) Injection current waveform

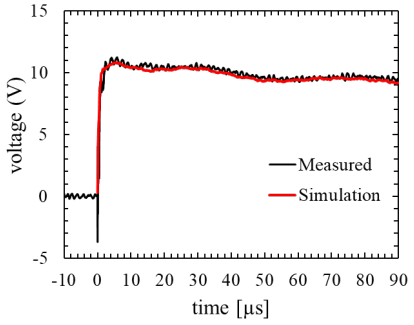

(b) Potential rise waveform

Fig. 13. Comparison of experimental results and analysis results when current is injected into the single model of the wind turbine No. 1.

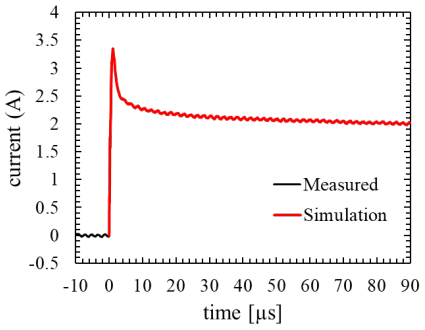

(a) Injection current waveform

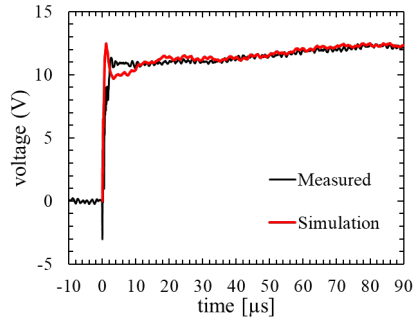

(b) Potential rise waveform

Fig. 14. Comparison of experimental results and analysis results when current is injected into the single model of the wind turbine No. 2.

To determine whether a highly accurate lightning surge analysis model has been constructed, it is essential to demonstrate that the analytical results closely match the experimental results, particularly in the wavefront. Therefore, in Fig. 13 and 14, experimental results focusing on the wavefront were obtained and compared with the analytical results. The comparison confirmed that the wavefront also exhibited a high degree of agreement.

B. Grounding wire model

The cross-sectional area of the grounding wire used in the experiment is 60 mm^2, and its parameters are shown in Table 1. As a first step in including this cable in the ATP program, the electrical parameters, such as the relative permittivity of the insulation layers and the electrical resistivity of the cores and sheath, were set to match the capacitance and resistance per km given by the manufacturer. This resulted in values of 4 for the cable internal insulation relative permittivity, and of 2.354×10^{-8} Ωm for the core's electrical resistivity. Fig.15 shows the external appearance of the grounding wire.

The grounding wire was modeled using the frequency-dependent transmission line model (JMarti [5]) available in ATP. In this model, a frequency band from 50 Hz to 1 MHz was used.

Based on this setup, the internal calculation option available in ATPDraw [12] was used for cable parameter calculation, which gave the most accurate results. This option aims to provide some alternative routines besides the already existent Line Cable Constants – LCC in ATP.

TABLE I
Parameters of the grounding wire

Parameter	CORE
Conductor radius (m)	0.005
Total radius (m)	0.007
Resistivity (Ωm)	2.354×10^{-8}
Insulation permittivity	4

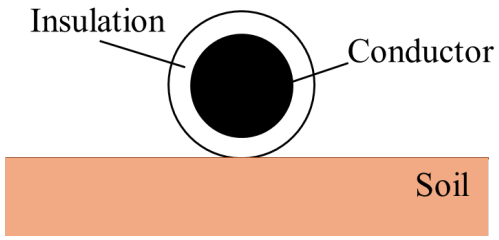

Fig. 15. Experimental layout when current is injected into wind turbine No.1

C. Model of connected wind turbines

Using the model constructed in the previous section, an analytical model was developed for the case where two wind turbines are interconnected with a grounding wire. The circuit diagram for this case is shown on Fig. 16. This circuit diagram is configured under the same conditions as in Fig. 6. The grounding conductor connected between wind turbines is artificially grounded on the surface. The tower section of the wind turbines is modeled as a 50-meter single-phase transmission line. In experiments where this kind of steep current is injected into the wind turbine foundation, a surge phenomenon appears at the wave front, which propagates above the wind turbine, reflects off the blade tips and the tower top, and returns to the tower bottom. single-phase transmission line model in ATP is a good and simple way to simulate this phenomenon.

Based on this complete model, simulations were performed to obtain the transient ground characteristics on the wind turbine No.1 side and the lightning current flowing in the ground wire when an impulse current is injected into wind turbine No.1.

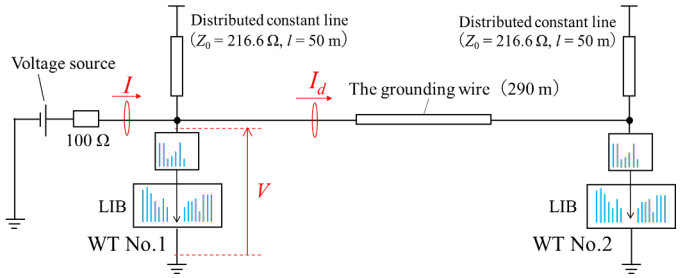

Fig. 16. Two Wind turbines connected model. (The LIB components correspond to the RLC equivalent circuit obtained from the Vector Fitting routine. The name of the interconnection node to the external circuit is defined internally).

Fig. 17 compares the experimental results with the simulation results. As shown in (a), the injected current is accurately transmitted to the wind turbine foundation. It can also be seen in the potential rise waveform in (b), which accurately reproduces the experimental results. However, in the shunt current waveform in (c), there is a discrepancy of about 20% at the wavetail. The main cause of this discrepancy is believed to be the failure to accurately model the soil between the turbines. Nevertheless, the shape of the waveform showed results that were very close to the experimental data.

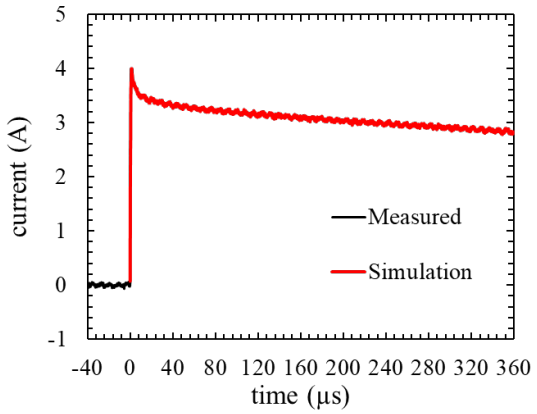

(a) Injection current waveform

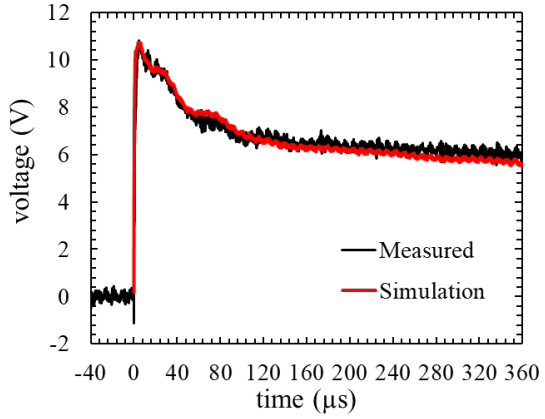

(b) Potential rise waveform

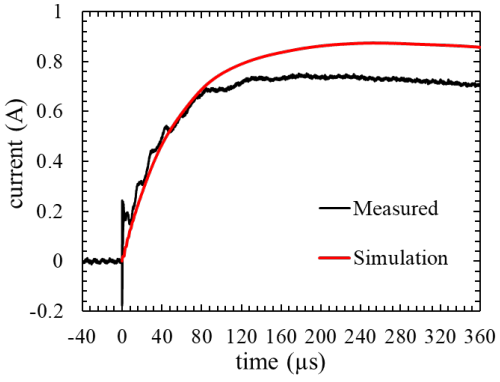

(c) Shunt current waveform

Fig.17. Comparison of experimental results and analysis results when two wind turbines are connected

IV. Verification of Methods to Reduce Lightning Current Flowing into Power Cable Sheaths

In this chapter, we inserted a power cable model into the analysis model presented in Chapter 3 and examined the

extent to which the ground wire between the wind turbines can reduce the current flowing into the power cable sheath.

As shown on Fig. 18, there have been reports of damage occurring due to a portion of the lightning current flowing into the cable sheath. The power cable model [13] was applied to the model constructed in Chapter III to analyze the distribution characteristics of lightning current flowing into the cable sheath, depending on the presence or absence of a grounding wire.

A. Analysis conditions

First, the cable model used for validation is explained. In this study, a model constructed in previous research was employed. The parameters of the cable and the pipe (such as conductor diameter and conductivity) were modeled using the same values as those in Reference [13]. Additionally, the surrounding ground was represented using the measurement results shown in Fig. 2. The three single-core cables were positioned 3 cm from the center of the pipe, as shown in Fig. 19.

Fig. 18. Power cable damaged by lightning

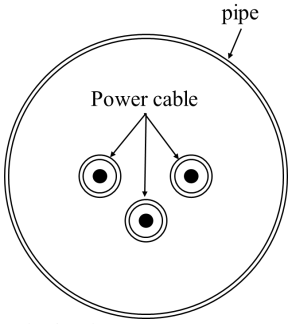

Fig. 19. Cable location in the pipe

Based on this configuration, the cable set was modeled using the frequency-dependent transmission line model available in ATP. In addition, the three cables were modeled in a twisted configuration.

A simplified schematic of the simulation circuit is shown in Fig. 20. In this figure, the current $I(t)$ is injected at the base of wind turbine No.1. The turbine and cable sheaths are connected to the same grounding system of the wind turbine. When the

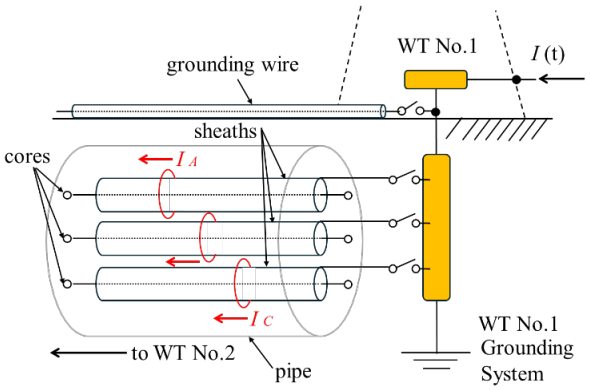

Fig. 20. Schematic of the simulation circuit

current is injected, the currents flowing through each cable sheath (I_A, I_B and I_C) are measured.

Additionally, the grounding wire described in Chapter II was laid on the ground surface. The influence of this grounding wire was examined to determine the extent to which it could mitigate the lightning current diverted into the cable sheaths.

B. Analysis results

The calculated results of lightning current flowing into the cable sheaths (all three phases grounded) are shown in Fig. 21. The waveforms presented in the figure represent the current flowing into each cable sheath individually. The waveform for the case without a grounding wire is shown in blue, while the waveform for the case with a grounding wire is shown in red. The injected current waveform is identical to that in Fig. 17(a).

From the results in Fig. 21, the calculated current at 360 μs is 0.33 A without the grounding wire and 0.20 A with the grounding wire. These results demonstrate that installing a grounding wire between wind turbines can reduce the lightning current flowing into the cable sheaths by approximately 39% per phase.

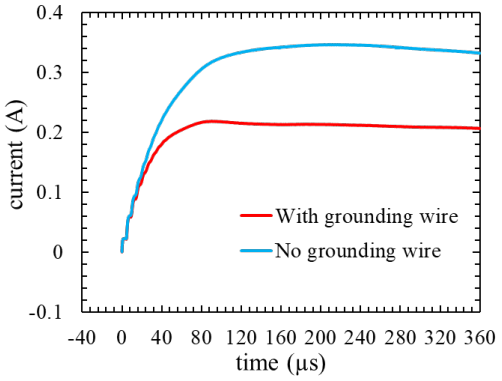

Fig. 21. Current flowing through the power cable (1 phase)

V. CONCLUSIONS

This paper presented the development of a wind farm model using ATP and a method to mitigate lightning current flowing into power cable sheaths.

For the grounding system of two wind turbines, a high-

accuracy model was successfully developed by calculating the frequency characteristics obtained from experimental results and applying the vector fitting method. It was found that the grounding wire model was highly sensitive to changes in its electrical and geometrical parameters. However, the model presented in this study is considered the most reliable version, as it incorporates parameters derived from actual experimental conditions and manufacturer specifications.

Additionally, as a method to reduce the lightning current flowing into cable sheaths, it was confirmed that installing grounding wires near the cables could reduce the lightning current by up to 39% per sheath. Furthermore, increasing the number of grounding wires is expected to further enhance the reduction effect. It is hoped that these findings will be utilized in future lightning protection measures.

Numerical electromagnetic field analysis such as FEM (Finite Element Method) and FDTD (Finite Difference Time Domain) methods have been used to simulate the detailed characteristics of wind turbine grounding systems. However, it is difficult to accurately model the arrangement and shape of the grounding electrodes in the soil, and it is also difficult to obtain information of accurate soil resistivity. As a result, the grounding characteristics analytically derived from the numerical electromagnetic field analysis model often do not match the actual grounding characteristics. In addition, the numerical electromagnetic field analysis method requires significantly longer calculation time than the circuit analysis model introduced in this paper. This approach offers a much simpler alternative to more computationally intensive methods like FEM or FDTD, which require detailed discrete modeling of the grounding system.

VI. References

[1] NEDO New Energy Department, “Wind Power Generation in Japan: Status of Wind Power Facilities and Installation Results,” New Energy and Industrial Technology Development Organization. [Online]. Available: https://www.nedo.go.jp/library/fuuryoku/state/1-01.html

[2] K. Yamamoto and S. Yanagawa, “Transient grounding characteristics of wind turbines,” in 2012 International Conference on Lightning Protection (ICLP), Vienna, Austria: IEEE, Sep. 2012, pp. 1–5

[3] K. Yamamoto, S. Yanagawa, K. Yamabuki, S. Sekioka, and S. Yokoyama, “Analytical Surveys of Transient and Frequency-Dependent Grounding Characteristics of a Wind Turbine Generator System on the Basis of Field Tests,” IEEE Trans. Power Delivery, vol. 25, no. 4, pp. 3035–3043, Oct. 2010,

[4] Nobuyuki Honjyo and Yoshimi Fukuda, “Report of lightning strike at Minami-Ehime Wind Power Plant,” 2020, Japan Wind Energy Society

[5] EMTP Leuven Center, Alternative Transients Program (ATP): Rule Book. EMTP, 1992

[6] B. Gustavsen and A. Semlyen, “Rational approximation of frequency domain responses by vector fitting,” IEEE Trans. Power Delivery, vol. 14, no. 3, pp. 1052–1061, Jul. 1999,

[7] K. Yamamoto, T. Matumoto, T. Fukunaga, R. Alipio, “Measured and simulated impulse responses of the grounding systems of a pair of wind-turbines connected by a buried insulated wire” Electric Power Systems Research 213 (2022), www.elsevier.com/locate/epsr

[8] S. Visacro, "A Comprehensive Approach to the Grounding Response to Lightning Currents," in *IEEE Transactions on Power Delivery*, vol. 22, no. 1, pp. 381-386, Jan. 2007, doi: 10.1109/TPWRD.2006.876707

[9] L. Grcev and F. Dawalibi, "An electromagnetic model for transients in grounding systems," in IEEE Transactions on Power Delivery, vol. 5, no. 4, pp. 1773-1781, Oct. 1990, doi: 10.1109/61.103673.

[10] A. Ubolli and B. Gustavsen, “A digital filtering approach for Time Domain Vector Fitting,” in 2011 IEEE 15th Workshop on Signal Propagation on Interconnects (SPI), Naples, Italy: IEEE, May 2011, pp. 25–28

[11] B. Gustavsen, “Passivity assessment and enforcement utilizing eigenpairs information,” Electric Power Systems Research, vol. 194, p. 107041, May 2021

[12] H. K. Høidalen, “ATPDraw - Graphical Processor for the ATP/EMTP.” http://www.atpdraw.net

[13] J .Herrera-Murcia, Y. Toriyama, K. Yamamoto“Distribution of lightning currents in underground interconnection cables for wind tuebines facilities”, International Conference on Grounding & Lightning Physics and Effects, pp. 139-144 (2024)